

Reverse Thrust Performance of a Variable-Pitch Fan Engine at Forward Velocity

D. C. Reemsnyder* and D. A. Sagerser*
NASA Lewis Research Center, Cleveland, Ohio

A variable-pitch fan engine was tested in the Ames 40 × 80 ft wind tunnel to determine the effect of forward velocity and crosswind on reverse-thrust performance. Two flight-type inlet configurations were tested, and a flared fan nozzle was installed as an inlet for reverse-thrust operation. Steady-state reverse-thrust performance was obtained up to 54 m/s (105 knots). An abrupt decrease in reverse thrust occurred at about 30 m/s (60 knots). Reverse thrust was established following forward-to-reverse thrust transients both statically and with forward velocities up to 30 m/s.

Nomenclature

A_{te}/A_D	= exlet trailing edge to fan duct area ratio
M_D	= fan duct Mach number
N	= fan speed, rpm
P_s	= local static pressure
P_{se}/P_{T0}	= exlet wall static pressure (internal)
P_{Si}/P_{T0}	= static pressure in fan inlet
P_{T0}	= tunnel total pressure
P_{T1}/P_{T0}	= exlet total-pressure recovery
P_{T2}/P_{T1}	= fan pressure ratio (reverse)
$P_{T2.5}/P_{T0}$	= core compressor total-pressure recovery (including exlet)
R_F	= fan radius at leading edge
V_o	= tunnel velocity
x	= axial distance from inlet highlight
α	= model angle of attack
β	= fan blade angle at 3/4 radius
$\Delta\beta$	= relative fan blade angle, i.e., angle from design forward blade angle
θ	= ratio of total temperature to standard sea-level temperature

Introduction

VARIABLE-pitch fan engines may be attractive for future short-haul aircraft if sufficient reverse thrust is available for aircraft deceleration after touchdown. Thrust reversal is obtained in these engines by changing fan blade pitch about 90 deg, which causes the fan airflow to enter the fan duct nozzle and exhaust through the fan inlet. This capability would eliminate the heavy and costly thrust reverser systems required for current fixed-pitch turbofan engines. The NASA Lewis Research Center has supported the development of advanced technology for a quiet, clean, high-bypass-ratio turbofan engine for future short-haul aircraft. A major portion of this effort is the Quiet, Clean, Short-Haul Experimental Engine (QCSEE) Program.¹ Previous work related to reverse-thrust operation of variable-pitch fan engines is summarized in an earlier paper.²

Presented as Paper 79-0105 at the AIAA 17th Aerospace Sciences Meeting, New Orleans, La., Jan. 15-17, 1979; submitted Feb. 15, 1979. This paper is declared a work of the U.S. Government and therefore is in the public domain. Reprints of this article may be ordered from AIAA Special Publications, 1290 Avenue of the Americas, New York, N.Y. 10019. Order by Article No. at top of page. Member price \$2.00 each, nonmember, \$3.00 each. **Remittance must accompany order.**

Index categories: Airbreathing Propulsion; Engine Performance; Aerodynamics.

*Project Engineer, Energy Conservative Engines Office. Member AIAA.

As part of the program to develop the propulsion system technology for short-haul aircraft, NASA has also supported testing of Hamilton Standard's Q-Fan T-55 engine. This engine features a full-size, dynamically controllable, variable-pitch fan. Previous tests,³⁻⁶ conducted on outdoor static-test rigs, have investigated steady-state reverse-thrust performance, and dynamic performance during forward-to-reverse thrust transients. During the tests,⁶ no difficulty was experienced in establishing reverse thrust with a bellmouth inlet for either engine startups with the fan blades in a fixed reverse-thrust position, or for forward-to-reverse thrust transient tests. However, with a flight-type inlet (smaller outlet area in reverse thrust), it was more difficult to establish reverse thrust both for startups and for transients.

Some difficulty in establishing reverse thrust during startup was also observed during reverse-thrust tests of a model of the QCSEE fan with a flight-type inlet.⁷ At some reverse-thrust blade angles the fan would initially be in a stalled condition at startup. Then, as speed was increased stall would clear and reverse thrust would be generated. The speed at which stall cleared was found to be a function of the preset reverse-fan blade angle. In both the Q-Fan T-55 engine tests and the QCSEE fan model tests, increasing the reverse fan blade angle (toward flat pitch) helped the fan to clear stall and establish reverse thrust.

To increase the technical knowledge of variable-pitch fans, an investigation into the effect of forward velocity and crosswind on reverse-thrust performance of the Q-Fan T-55 engine was conducted in the NASA Ames 40 × 80 ft wind tunnel. The test objectives were to determine the effect of forward velocity and crosswind on steady-state reverse-thrust performance, to determine the effect of forward velocity on forward-to-reverse thrust transient performance, and to determine the effectiveness of an overshoot blade angle technique to establish the reverse thrust during a transient. Tunnel velocities during the tests were set from 0 to 54 m/s (105 knots). The model angle of attack was varied from 0 deg to 22 deg to simulate crosswind. Maximum fan speed was 3255 rpm (97.5% $N/\sqrt{\theta}$). And the fan blade angle range was 43 deg (forward) to 168 deg (reverse through feather pitch).

Apparatus and Procedure

Details of the instrumentation, data reduction, and test procedure are discussed in Ref. 8.

Test Facility

A photograph of the engine installed in the wind tunnel is shown in Fig. 1. The engine with nacelle was mounted on a single, hollow-column pylon approximately 3.8 m (150 in.) from the wind-tunnel floor. The pylon, in turn, was attached

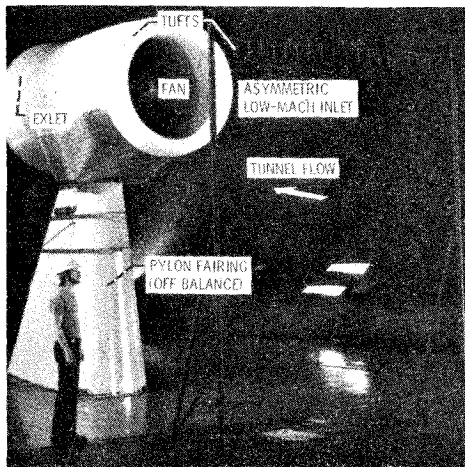


Fig. 1 Q-Fan T-55 engine installed in Ames 40 × 80 ft wind tunnel.

to the floor-mounted turntable located on the wind tunnel vertical centerline. The turntable, strut, and nacelle were "on balance" for measuring model forces. A large fairing, or "wind shield," off balance, protected the turntable and strut surfaces from the wind-tunnel aerodynamic forces. The nacelle was yawed in the horizontal plane by means of the tunnel turntable to simulate operation at the various inlet angles of attack. The inlet top to bottom (0 deg to 180 deg) axis was located on the horizontal plane of the wind tunnel. White tufts were installed on a wire on the engine horizontal centerline about 3.0 m (10 ft) in front of the engine inlet highlight and on the external surface of the low-Mach inlet nacelle (Fig. 1).

Engine Test Configuration

The test model consisted of an inlet, a variable-pitch fan, a gas-turbine core engine, an exlet (reverse flow inlet), and appropriate fairings, nozzles, etc. The Hamilton-Standard Q-Fan demonstrator is a 1.397-m (55-in.), 13-bladed, variable-pitch fan with a Lycoming T-55-L-11A, 2796-kW (3750-hp) gas-turbine core engine. A schematic of the Q-Fan T-55 engine showing the major components and the instrumentation station designations is shown in Fig. 2. The engine has a 17:1 bypass ratio and is driven through a 4.75:1



Fig. 3 Fan blade angle convention. a) forward thrust; b) reverse thrust through feather (stall) pitch.

gear reduction to a maximum speed of 3365 rpm. The fan has a 0.645-m (25.4-in.) diameter, semielliptical nose dome fairing. The fan exit nozzle was an annulus with an exit area of 1.064 m² (1649 in²). The reverse-thrust exlet with a 30 deg (half angle) conical flare was mounted on the aft end of the fan exit nozzle for reverse-thrust operation.

A schematic of the variable-pitch fan blade in the forward and the reverse-through-feather pitch configurations is shown in Fig. 3 with the blade-angle convention noted. In the reverse-through-feather configuration the blade camber correctly turns the flow toward axial, but the leading and trailing edges are reversed.

Two flight-type inlets were tested with the Q-Fan T-55 engine. The Boeing Lift/Cruise low-Mach inlet had an asymmetric inlet contour with the windward side having a higher contraction ratio (1.76) than the leeward side (1.30). At a given inlet station both the internal and external contours are of circular cross section with offset centers. The high-Mach inlet was geometrically similar to the QCSEE inlet, which was designed with a high throat Mach number (0.79) for fan inlet noise suppression. Because of the smaller inlet throat diameter, the high-Mach inlet has a ratio of inlet throat to fan face flow area of 0.81, as compared with 0.93 for the low-Mach inlet. The average inlet throat to fan diameter ratio was 0.80 for the high Mach inlet and 0.855 for the low Mach inlet.

Data Reduction

Steady-state reverse-thrust data reduction included the calculation of the following parameters: (1) corrected tunnel and force balance parameters, (2) measured corrected engine reverse thrust along engine centerline, (3) fan speed, (4) fan average total- and static-pressure ratios, (5) aft fan duct airflow, (6) exlet (fan duct) total-pressure recovery and distortion, (7) core engine speed, torque, and power, and (8)

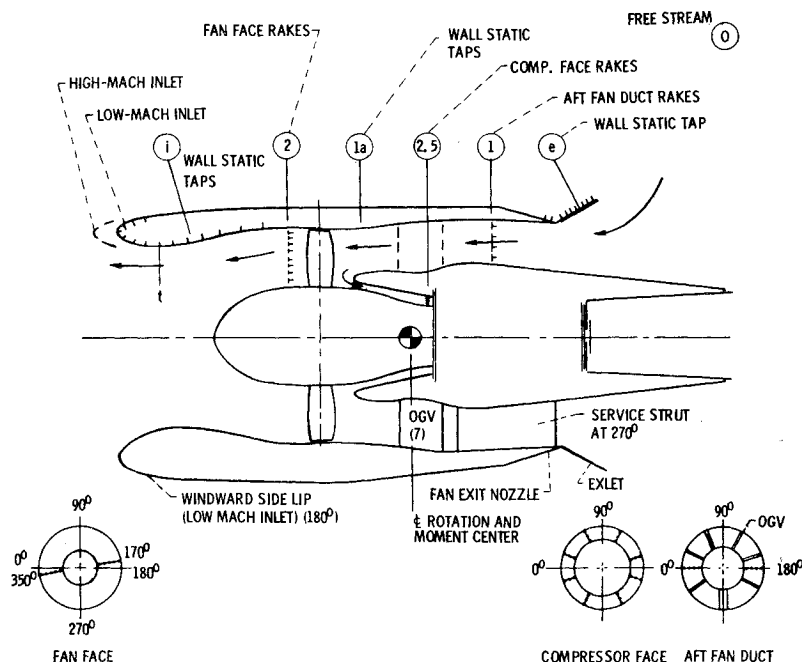


Fig. 2 Q-Fan T-55 engine reverse-thrust configuration.

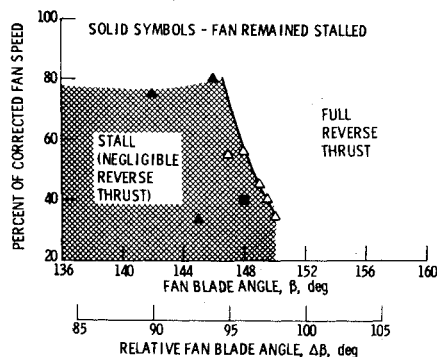


Fig. 4 Fan stall-to-unstall transition speed. (Fan speed increased at constant β at startup.) Static conditions; low Mach inlet.

core compressor airflow, total and static pressures, distortion, and total-pressure recovery.

Forward-to-reverse thrust transient data reduction consisted of digitizing the analog data from magnetic tapes (about 30 data points per average) to produce a data point for each 0.01 s from the start to end of the transient. Calculated parameters throughout the transient include fan blade-angle position and rate, corrected fan and core speeds, corrected core engine torque and power, fan static-pressure ratios and differences, fan blade stresses, and dynamic pressure fluctuations. Calculated values for each successful transient include actual overshoot blade angle, dwell time, total thrust response time, actual blade travel time, and flow reattachment time.

Steady-State Reverse-Thrust Performance

Reverse-thrust performance was obtained with the engine and the wind tunnel at steady-state operating conditions. Operational boundary conditions were determined with relatively slow changes in either fan blade angle or fan speed. Performance is presented here for the low Mach inlet only.

Reverse-Thrust Starting and Stall-Unstall Characteristics at Static Conditions

To better understand the starting and stall-unstall characteristics of this fan, a number of manually controlled variations in fan speed and fan blade angle were conducted to determine the conditions where reverse thrust was established or lost. These quasi-steady-state results, which can also be obtained in model fan tests, may be correlated with forward-to-reverse thrust transient performance.

All engine startups for reverse-thrust performance were attempted with a preset reverse fan blade angle under static (tunnel off) conditions. Results of the tests are shown in Fig. 4. With a fan blade angle of 150 deg, reverse thrust was observed at the lowest stabilized fan speed. With low fan blade angles from 147 to 149.5 deg, the fan was stalled initially, and fan speed had to be increased to clear stall and establish reverse thrust. An abrupt transition occurred from the fully stalled, negligible reverse-thrust mode to the unstalled reverse-thrust mode. Considerable hysteresis was also observed in that once reverse thrust was established; no transitions were observed back to the fully stalled mode by decreasing fan speed. At a fan blade angle of 146 deg reverse thrust could not be established even up to 81% fan speed. The high-Mach inlet had similar characteristics, but the smaller effective outlet throat area in reverse made it more difficult to establish reverse thrust. Unstalling of the fan by increasing fan speed at some reverse fan blade angles and not returning to a stalled condition when decreasing fan speed was also observed during reverse-thrust tests of a model of the QCSEE variable pitch fan.⁷

In the above cases where the fan remained stalled during startup, reverse thrust could be established by increasing fan

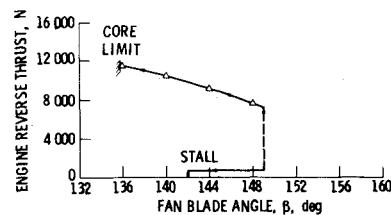


Fig. 5 Reverse-thrust hysteresis with fan blade angle. Low Mach inlet; 75% $N/\sqrt{\theta}$.

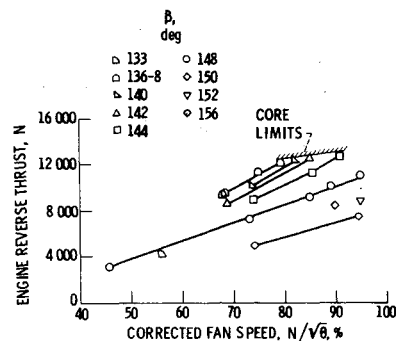


Fig. 6 Q-Fan T-55 engine steady-state reverse-thrust performance with low Mach inlet; static conditions.

blade angle at a constant fan speed. A typical example of the reverse-thrust hysteresis with fan blade angle is presented in Fig. 5 at 75% of fan speed. Negligible reverse thrust was observed initially as β was increased from 142 to 149 deg, the engine abruptly changed to the full reverse-thrust mode. Reverse thrust increased as β was then decreased to 136 deg, where core speed and turbine temperature limits were encountered. Once reverse thrust was established at 149 deg, the fan blade angle could be varied considerably (± 10 to ± 15 deg) without the engine reverting to the fully stalled mode, indicating a large hysteresis in performance with fan blade angle. It should be noted that the desired blade angle operating range is below 149 deg to obtain high reverse thrust. But operation at these low blade angles may be impossible without first establishing reverse thrust at higher fan blade angles. Reverse-thrust testing of a variable-pitch fan and inlet combination may therefore require a means of adjusting β during fan operation to obtain high values of reverse thrust.

Reverse-Thrust Performance at Static Conditions

Steady-state reverse-thrust performance at static conditions (tunnel off) is presented in Fig. 6 at various reverse-fan blade angles and fan speeds. To obtain these data, reverse thrust was initially established by either increasing fan speed or fan blade angle. Performance trends at static conditions are similar to those obtained in previous tests of this engine.³ Reverse thrust increases with increasing fan speeds and with decreasing reverse-fan blade angles down to 136 deg. At the lower fan blade angles, high fan speeds could not be obtained because of core speed and turbine temperature limits, as noted in the figure.

Effect of Forward Velocity on Reverse-Thrust Performance

Previous steady-state reverse-thrust testing of the Q-Fan T-55 engine in outdoor static-test stands showed that the engine could operate in one of two modes: a full reverse-thrust mode and a negligible reverse-thrust, stalled-fan mode. During the wind-tunnel tests with forward velocity, a third, partial reverse-thrust mode was observed. The partial reverse-thrust mode was characterized by lower reverse thrust and negligible fan jet penetration into the freestream than the full reverse-thrust mode. During the wind-tunnel tests the engine would abruptly change from the full reverse-thrust mode to the

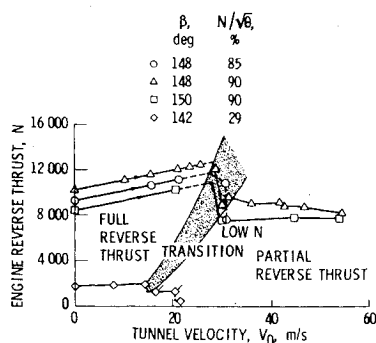


Fig. 7 Effect of increasing tunnel velocity on steady-state reverse-thrust performance; low Mach inlet; $\alpha = 0$ deg.

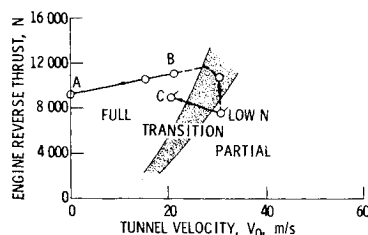


Fig. 8 Reverse-thrust hysteresis loop with tunnel velocity. Low Mach inlet; $\alpha = 0$ deg; $\beta = 148$ deg; $N/\sqrt{\theta} \sim 85\%$.

partial reverse-thrust mode as the tunnel velocity was increased at constant engine power setting. Once the engine shifted from the full to the partial reverse-thrust mode, considerable hysteresis was associated with reverting to the full reverse-thrust mode. As subsequent figures will show, the fan remained stable and did not stall during the transition from full to partial reverse thrust, but significant changes in static pressures (and forces) on the inlet and exlet occurred.

The effect of increasing forward velocity on reverse-thrust performance with the engine set at a fixed fan blade angle and fan speed is presented in Fig. 7. Generally, it can be seen that as tunnel velocity increases reverse thrust increases until a point where the engine abruptly changes to a partial reverse-thrust mode. This transition appears to be a function of fan speed, as noted in the figure. The transition to the partial reverse-thrust mode occurred at about 30 m/s and resulted in a significant ($\sim 30\%$) decrease in reverse thrust, a slight ($\sim 5\%$) decrease in fan speed, and negligible fan jet penetration to the tufts. Fan speed was readjusted to the initial value by increasing the engine power setting and the tests were continued at constant N and β . The engine operated satisfactorily in the partial reverse-thrust mode with a gradual decrease in reverse thrust to a forward velocity of 54 m/s. In the wind-tunnel tests of a 50.8-cm fan model,⁹ reverse thrust decreased gradually with increasing tunnel velocity from static up to 43 m/s. No abrupt transition was noted. About 50% of the static reverse thrust was measured at a tunnel velocity of 41 m/s (80 knots).

A typical reverse-thrust hysteresis loop with tunnel velocity is shown in Fig. 8 for a β of 148 deg at 85% of fan speed. It should be noted that, once the engine transitioned to the partial reverse-thrust mode, tunnel velocity could be reduced to less than 20 m/s (below the transition zone) without reverting to the full reverse-thrust mode.

Analysis of Forward Velocity Effects

To help understand the effect of forward velocity and the transition from the full to the partial reverse-thrust mode, several more detailed performance characteristics were examined at conditions A, B, and C (Fig. 8). Point A is the static condition, point B is full reverse thrust at 20 m/s, and point C is partial reverse thrust at 20 m/s. Points A, B, and C are all at a β of 148 deg and a fan speed of 85%. No changes

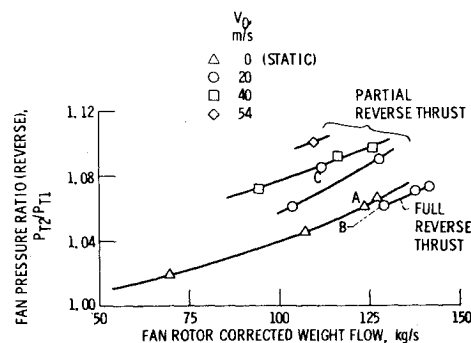


Fig. 9 Steady-state reverse-thrust fan performance at several forward velocities. Low Mach inlet; $\alpha = 0$ deg; $\beta = 148$ deg.

in the exlet or core total-pressure recovery were observed that would account for the transition from the full to the partial reverse-thrust mode (from point B to C). The effect of tunnel velocity on the 30 deg conical exlet total-pressure recovery is similar to that obtained with a 14-cm (5.5 in.) diameter exlet model.¹⁰

The fan performance map for the steady-state reverse-thrust tests is presented in Fig. 9 for $\beta = 148$ deg at various tunnel velocities. The static (tunnel off) fan operating line is shown for reference. A slightly lower than static fan operating line (OL) was observed at a forward velocity of 20 m/s in the full reverse-thrust mode. Measured fan rotor flow increased about 5% at constant fan speed. A significantly higher fan operating line is observed at 20 m/s in the partial reverse-thrust mode as compared with the full reverse-thrust mode. This shift in fan OL correlates with the sudden change in reverse thrust from the full to the partial reverse-thrust modes. However, the decrease in ideal fan reverse thrust from point B to C is significantly less than the measured change in thrust. Ideal fan reverse thrust is based on fan flow, fan outlet pressure, and tunnel velocity (ram drag). In the partial reverse-thrust mode, increasing forward velocity up to 54 m/s caused the fan OL to move even higher, indicating evidence of a back pressure effect on the fan due to the increased forward velocity. Fan-inlet and -outlet pressure profiles were similar for conditions A, B, and C, which indicates that the change in the fan operating line was apparently due to flow changes external to the fan.

Since pressure forces on the flared exlet can be very large and directly affect the net reverse thrust, the axial static pressure distribution along the exlet internal surface is shown in Fig. 10. In the full reverse-thrust mode at 20 m/s (condition B), static pressures were significantly lower than those measured at static conditions (A), indicating a large increase in the exlet's contribution to reverse thrust. The transition

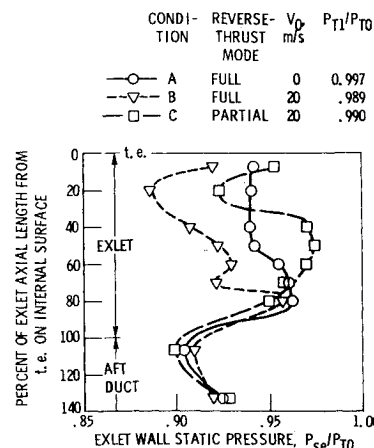


Fig. 10 Exlet axial static-pressure distribution, windward side; $\beta = 148$ deg; $N/\sqrt{\theta} \sim 85\%$, $A_e/A_D = 2.0$; $M_D \sim 0.33$.

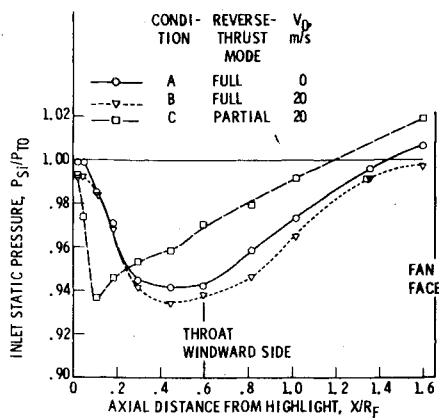


Fig. 11 Inlet axial static-pressure profiles. Low Mach inlet, windward side; $\beta = 148$ deg; $N/\sqrt{\theta} \sim 85\%$. Tunnel $P_S/P_{T0} = 0.997$ at 20 m/s.

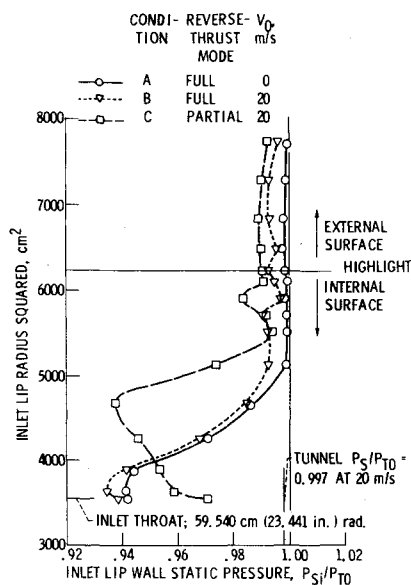


Fig. 12 Inlet lip wall static-pressure radial profile. Windward side; $\beta = 148$ deg; $N/\sqrt{\theta} \sim 85\%$.

from the full to partial reverse-thrust mode at 20 m/s (condition B to C) is characterized by a significant increase in the exlet static pressure, indicating a large decrease in the exlet's reverse-thrust contribution. This change in pressure was also evident when full and partial reverse-thrust mode points were compared at equal flow rates, which suggests that a change occurred in the engine external flowfield. Variations in the exlet static pressure forces correlate very well with the variations in measured reverse thrust at the three conditions compared.

The axial static-pressure distribution is presented for the windward thick-lip side of the inlet in Fig. 11. Similar characteristics were observed on the thin-lip side of the inlet. At 20 m/s in the full reverse-thrust mode (condition B), the inlet surface static-pressure profile differs only slightly from that obtained at static conditions (condition A). However, in the partial reverse-thrust mode at the same forward velocity (condition C), the location of the minimum static pressure moved significantly forward of the throat, and the level of static pressures increased significantly between the minimum pressure and the fan face. The significantly higher static pressure at the inlet throat results in the higher fan operating line.

Since inlet lip pressure forces can be very large and directly affect the net reverse thrust, the inlet static pressure data from Fig. 11 is plotted versus inlet lip projected area in Fig. 12 for the windward, thick-lip side of the inlet. Similar charac-

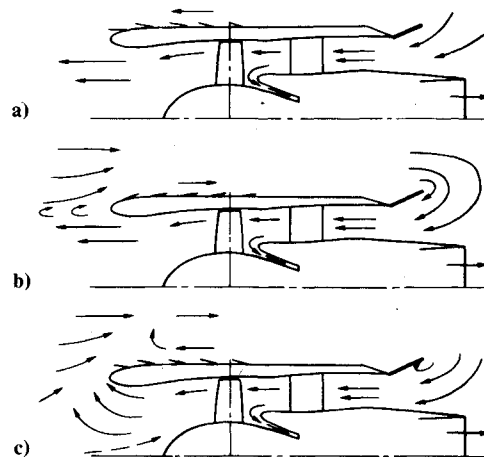


Fig. 13 Reverse-thrust flow patterns. $\beta = 148$ deg; $N/\sqrt{\theta} \sim 85\%$. a) static; b) full reverse thrust at 20 m/s; c) partial reverse thrust at 20 m/s.

teristics were observed on the thin-lip side of the inlet. Again, inlet radial profiles are very similar at static conditions and at 20 m/s in the full reverse-thrust mode. In the partial reverse-thrust mode at 20 m/s, the inlet radial profile shifted considerably, resulting in significantly lower lip static pressures, which have a decreasing effect on reverse thrust. The location of the minimum static pressure moved significantly outward radially, which suggests that the flow is tending to follow the lip contour radially outward rather than separate near the throat as it apparently did in the full reverse-thrust mode.

A schematic of the flow through the engine statically and at 20 m/s in the full and partial reverse-thrust modes is presented in Fig. 13. Flow directions are based on photographs of the tufts on the external surface of the low-Mach inlet and of the line of tufts on the engine horizontal centerline 3.0 m (10 ft) in front of the inlet highlight, and on the previous analysis of engine performance. The primarily axial fan jet is shown for the static and full reverse-thrust mode conditions at 20 m/s. In the partial reverse-thrust mode at 20 m/s the fan jet flow is radially outward over the inlet lip. The nacelle surface tufts in the static and partial modes were predominantly forward, while in the full reverse-thrust mode they were predominantly rearward over the nacelle surface.

The previous analysis indicates a possible explanation of the abrupt transition from the full to the partial reverse-thrust mode at a forward velocity of about 30 m/s. The primary cause of the observed reduction in reverse thrust during the transition appears to be the result of significant changes in force on the nacelle due to the increasing forward velocity. In the partial mode the high static pressures on the exlet internal surface result in a significant decrease in the exlet's contribution to reverse thrust. Changes in surface flow on the inlet lip were observed, which would also contribute to decreased reverse thrust. It appears that the fan outlet flow is affected by the change in static pressure due to the increasing tunnel velocity, until the flow suddenly attaches, possibly due to the Coanda effect, to the inlet lip surface. The primarily axial fan jet then abruptly collapses and spills radially outward over the inlet lip, as indicated by the lower static pressures forward of the inlet throat. The corresponding higher inlet throat and fan-face pressures indicate a throttling effect on the fan, resulting in the observed higher fan operating line.

Reverse-Thrust Performance with Crosswind

Very limited data were obtained with angle of attack to simulate crosswind effects. Two cases of angle-of-attack variation on steady-state reverse thrust performance are presented in Fig. 14. Both tests were conducted at constant forward velocity with the engine initially in the partial reverse

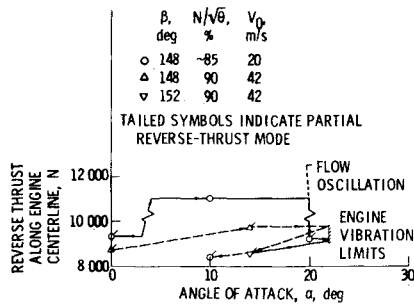


Fig. 14 Effect of angle of attack on steady-state reverse thrust at constant forward velocity; low Mach inlet.

thrust mode at 0 deg angle of attack. In one test at 20 m/s, angle of attack significantly affected reverse-thrust operation by causing the engine to abruptly change from the partial to the full reverse-thrust mode at a low angle of attack of about 3 deg, and then abruptly return to the partial reverse-thrust mode at about 20 deg. In the other test at a high forward velocity (42 m/s), no transition was observed from the partial to the full reverse-thrust mode. Severe buffeting and high engine vibrations occurred at angles of attack above 20 deg.

Forward-to-Reverse Thrust Transient Performance

All forward-to-reverse thrust transients were initiated from either an approach or takeoff forward-thrust engine operating condition. During static (tunnel off) operation, the engine in the forward-thrust mode induced a forward velocity up to 10 m/s at the initiation of the transient. All transients had the same programmed final reverse-thrust blade angle of about 149 deg and corrected fan speed of about 85%.

Initial Steady-State Forward-Thrust Performance

Steady-state forward thrust performance was obtained to define the initial takeoff, aborted takeoff, and approach engine operating conditions for the forward-to-reverse thrust transient tests. The reverse exlet appeared to have only a very slight effect on forward thrust performance.

The static takeoff condition was determined by operating the engine at the design fan blade angle (51.8 deg) and 95% fan speed with the tunnel off. The engine was operated at the same fan blade angle and fan speed at a forward velocity of 40 m/s for the aborted takeoff condition. A thrust level of 78% of the static takeoff thrust was measured at this aborted takeoff condition. The approach condition at 40 m/s was determined by operating at 95% of fan speed and varying fan blade angle until a thrust level equal to about 60% of that at the aborted takeoff condition was obtained. This condition was achieved at a fan blade angle of 44 deg.

Definition of Transient Terms

Terms for transient performance are shown in Fig. 15. Blade travel time (BT) is simply the time from the demand for reverse thrust until the fan blade comes within 1 deg of the overshoot blade angle. Dwell is the time the fan blade is held at the overshoot blade angle. Flow reattachment time (RAT) is the time it takes the airflow to reverse and reattach to the fan blades after the fan blades have reached within 1 deg of the overshoot blade angle. Fan blade stress was used to indicate when flow reattachment occurred. As observed in previous tests, fan blade stresses increase substantially during a transient and then suddenly drop when reverse thrust was established.⁶

For the forward-to-reverse thrust transient tests, the time required to establish reverse thrust (thrust response time) is the primary parameter of interest. For these tests the thrust-response time is simply the sum of BT and RAT. Since BT is only a function of the actuation rate and RAT is primarily an aerodynamic phenomena, transient performance will be presented here in terms of RAT and the factors that affect it.

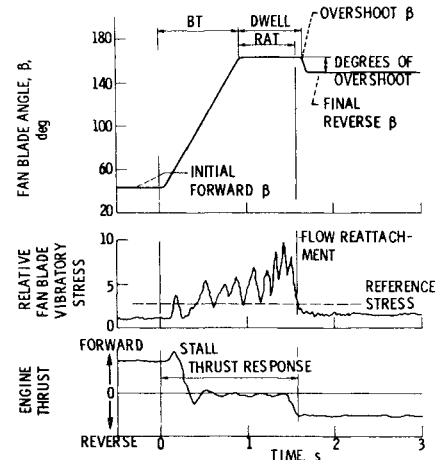


Fig. 15 Nomenclature for forward-to-reverse thrust transients.

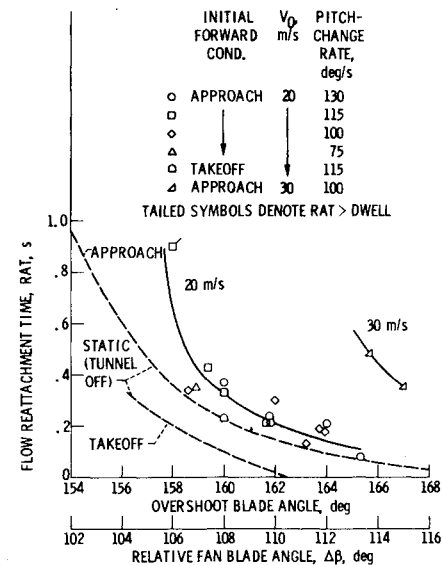


Fig. 16 Forward-to-reverse transient performance with forward velocity. Low Mach inlet. Dwell, 0.4 to 0.6 s.

Transient Performance with Low-Mach Inlet

Forward-to-reverse thrust transient performance with the low-Mach inlet at various forward velocities is presented in Fig. 16. Transient performance at static (tunnel off) conditions is represented by the dashed curves for approach and takeoff. Based on performance and tuft observations, all of the 20 attempted transients at static conditions were successful, with overshoot blade angles of 154 deg (minimum attempted) or greater. Some of these transients were initiated at forward velocities up to 10 m/s (20 knots). These velocities were induced by forward engine operation in the wind tunnel. As shown in the figure, increasing the overshoot blade angle results in decreasing RAT, a trend similar to that observed in previous tests with a bellmouth inlet.⁶ It should be noted that increasing overshoot blade angle increases BT, but this increase is small compared with the resulting decrease in RAT. At static conditions, RAT did not appear to be significantly affected by the blade pitch-change rate. Initiating the transient from the high-power takeoff condition resulted in decreased RATs and earlier establishment of reverse thrust.

For several data points, RAT exceeds dwell time. This means that the flow reattached after the blade was returned from the overshoot blade angle to the final reverse blade angle. Thus, an apparent aerodynamic lag as large as 0.4 s occurred after the blade returned to the final reverse blade angle. This aerodynamic lag is also evident in previous data.⁶

A reduction in RAT may have resulted if dwell time had been increased for these cases.

Forward-to-reverse thrust transients were attempted at forward velocities of 20, 30, and 40 m/s (40, 60, and 80 knots). With 20-m/s (40 knots) forward velocity, reverse thrust was established at most attempted conditions. Visual tuft observations and performance indicate that the engine, in most cases, was in a partial reverse-thrust mode after the transient. With the 40-m/s (80 knots) forward velocity, reverse thrust could not be established dynamically in four attempts (overshoot blade angles from 158 deg to the maximum available, 168 deg), and the fan remained fully stalled. Increasing the overshoot blade angle beyond the 168 deg actuator limit may not be effective in reducing RAT, since the blades would then be approaching the flat pitch position.

Reasonable flow reattachment times (<0.5 s) were obtained at a forward velocity of 20 m/s with an overshoot blade angle of 158.5 deg or greater. At an overshoot blade angle of 158 deg the RAT approached 1.0 s. Changing the initial forward operating condition from low power approach to high power aborted takeoff did not appreciably change the RAT. However, the aborted takeoff RATs were significantly longer at 20 m/s than those with the tunnel off.

With 30 m/s forward velocity, partial reverse thrust was established with overshoot blade angles of 166 deg or greater, but with longer RATs than comparable data at lower forward velocities. As noted in Fig. 16, forward velocity requires overshoot blade angle to be increased to maintain acceptable flow reattachment times.

Successful transients with the high-Mach inlet required higher overshoot blade angles than with the low-Mach inlet. This result correlates with the effect of the high-Mach inlet on the unstalling fan blade angle (discussed previously), suggesting that this inlet has a similar back pressuring effect on the stalled fan in both tests. As noted with the low-Mach inlet, RATs increased rapidly with decreasing overshoot blade angle.

Summary of Results

Reverse-thrust performance of the variable-pitch, Q-Fan T-55 engine was obtained in the NASA Ames 40×80 ft wind tunnel at tunnel velocities up to 54 m/s (105 knots) and at angles of attack up to 22 deg.

Steady-State Reverse-Thrust Performance

1) The Q-Fan T-55 engine started at static conditions with the fan in either a stalled or unstalled mode dependent on the preset reverse-thrust fan blade angle. If initially stalled, reverse thrust was established by increasing fan speed or by increasing fan blade angle. It was more difficult to establish reverse thrust with the high-Mach inlet (smaller effective outlet throat area in reverse) than with the low-Mach inlet.

2) During the wind-tunnel tests with forward velocity, an unexpected partial reverse-thrust mode was observed with both flight-type inlets. The transition from full to partial reverse thrust occurred abruptly as the tunnel velocity was increased to about 30 m/s (60 knots) with the engine power setting held constant. The partial reverse-thrust mode was characterized by significantly lower reverse thrust, a higher fan operating line, lower inlet lip and higher exlet static pressures, and negligible fan jet penetration into the free-stream as compared with the full reverse thrust mode. The primary cause of the observed reduction in reverse thrust in the partial mode appears to be the result of significant changes in pressure forces on the nacelle as forward velocity increased. Considerable hysteresis was associated with reverting to the full reverse thrust mode by decreasing tunnel velocity.

3) In the full reverse-thrust mode, reverse thrust increased, as expected, with increasing tunnel velocity up to about 30 m/s, and the primarily axial fan jet penetrated upstream.

4) Conversely, in the partial reverse-thrust mode, increasing forward velocity from about 20 to 54 m/s (40 to 105 knots) resulted in a gradual decrease in engine reverse thrust to about 80% of the initial static value. The fan operating line moved significantly higher with increasing forward velocity, whereas, it moved slightly lower in the full reverse-thrust mode. The fan outlet flow remained attached to the inlet lip and spilled radially outward.

5) Limited crosswind tests showed that in some cases variations in angle of attack caused the engine to change reverse-thrust modes (partial to full and full to partial). Buffetting and high-engine vibrations occurred at angles of attack above 20 deg.

Forward-to-Reverse Thrust Transient Performance

1) In the forward-to-reverse thrust transient tests, the overshoot blade angle technique proved effective in reducing the time required to establish reverse thrust with a flight-type inlet both statically and with forward velocity. Forward-to-reverse transients were accomplished only up to 30 m/s forward velocity with the low-Mach inlet and up to 20 m/s with the high-Mach inlet. Above 30 m/s reverse thrust could not be established.

2) Forward velocity requires higher overshoot blade angles in order to establish and maintain reverse thrust. Increasing the overshoot blade angle results in decreasing flow reattachment times and earlier establishment of reverse thrust both statically and with forward velocity. For example, transients with the low-Mach inlet required about 2 deg more overshoot blade angle at 20 m/s and 9 deg more overshoot blade angle at 30 m/s to achieve flow reattachment times equal to those obtained statically. The high-Mach inlet requires about 6 to 10 deg more overshoot blade angle than the low-Mach inlet under similar operating conditions. After all successful transients, except for some conducted at 20 m/s forward velocity, the engine operated in the partial reverse thrust mode.

3) Transients performed at static conditions (tunnel off) with high-power takeoff conditions had faster reattachment times than those with low-power approach conditions, but these differences tended to disappear with forward velocity. Blade pitch change rate did not significantly affect flow reattachment time at static conditions or with forward velocity. In some transient tests the flow reattached to the fan blade after the blade was returned from the overshoot blade angle to the final reverse blade angle. This aerodynamic lag was as long as 0.4 s.

Concluding Remarks

Short-haul aircraft landing or aborted takeoff maneuvers require successful deceleration from speeds of about 40 m/s (80 knots) or higher. During aircraft deceleration thrust reversal must be initiated and maintained consistently and repeatedly to prevent aircraft yawing due to dissimilar engine thrust levels. Forward velocity caused the variable pitch Q-Fan T-55 engine to operate in an unexpected partial reverse thrust steady-state mode under some operating conditions [e.g., above 30 m/s (60 knots)]. Full or partial reverse thrust was established following forward-to-reverse thrust transients only up to a forward velocity of about 30 m/s (60 knots).

However, these undesirable effects of forward velocity may be peculiar to this fan-nacelle configuration. The Q-Fan T-55 demonstrator engine had a very low (1.14) pressure ratio fan and a simple conical flared exlet. The observed characteristics may not be typical of similar higher pressure ratio fans. Furthermore, no attempt was made to modify the nacelle to reduce the adverse effects of forward velocity. Further development of advanced variable-pitch turbofan engines is therefore recommended to insure adequate and reproducible reverse-thrust levels for successful aircraft deceleration.

Acknowledgment

The authors are indebted to W. J. Demers and Hamilton-Standard for supplying and operating the test engine, the Boeing Company for data acquisition and reduction, and NASA Ames for operation of the wind tunnel and force balance and providing hardware and test support.

References

- ¹Ciepluch, C.C., "Quiet, Powered-Lift Propulsion," NASA Conference Publication 2077, Nov. 1978.
- ²Sagerser, D.A., Schaefer, J.W., and Dietrich, D.A., "Reverse-Thrust Technology for Variable Pitch Fan Propulsion Systems," *Powered-Lift Aeronautics and Acoustics*, NASA SP-406, 1976, pp. 387-402.
- ³Demers, W.J., Metzger, F.B., Smith, L.W., and Wainauski, H.S., "Testing of the Hamilton Standard Q-Fan Demonstrator," Hamilton Standard, Windsor Locks, Conn., HSER-6163, Vols. 1 and 2, 1973, NASA CR-121265.
- ⁴Demers, W.J., Nelson, D.J., and Wainauski, H.S., "Hamilton Standard Q-Fan Demonstrator Dynamic Pitch Change Test Program, Vol. 1," Hamilton Standard, Windsor Locks, Conn., HSER-6700-Vol. 1, 1975, NASA CR-134861.

⁵Demers, W.J., Nelson, D.J., and Wainauski, H.S., "Hamilton Standard Q-Fan Demonstrator Dynamic Pitch Change Test Program, Vol. 2," Hamilton Standard, Windsor Locks, Conn., HSER-6700-Vol. 2, 1975, NASA CR-134862.

⁶Schaefer, J.W., Sagerser, D.A., and Stakolich, E.G., "Dynamics of High-Bypass-Engine Thrust Reversal Using a Variable-Pitch Fan," NASA TM X-3524, 1977.

⁷Giffin, R.G., McFalls, R.A., and Beacher, B.F., "QCSEE Aerodynamic and Aeromechanical Performance of a 50.8 cm (20 in.) Diameter, 1.34 PR, Variable-Pitch Fan with Core Flow," General Electric Co., Cincinnati, Ohio, R75AEG445, Proj. FEDD, Aug. 1977, NASA CR-135017.

⁸Reemsnyder, D.C. and Sagerser, D.A., "Effect of Forward Velocity and Crosswind on the Reverse-Thrust Performance of a Variable-Pitch Fan Engine," AIAA Paper 79-0105, AIAA 17th Aerospace Sciences Meeting, New Orleans, La., Jan. 1979.

⁹Wesoky, H.L., Abbott, J.M., Albers, J.A., and Dietrich, D.A., "Low-Speed Wind Tunnel Tests of a 50.8-Centimeter (20-in.) 1.15 Pressure Ratio Fan Engine Model," NASA TM X-3062, 1974.

¹⁰Keith, T.G., Obee, T.N., and Dietrich, D.A., "Total Pressure Recovery of Flared Fan Nozzles Used as Inlets," *Journal of Aircraft*, Vol. 16, Feb. 1979, pp. 110-115.

From the AIAA Progress in Astronautics and Aeronautics Series . . .

INTERIOR BALLISTICS OF GUNS—v. 66

*Edited by Herman Krier, University of Illinois at Urbana-Champaign,
and Martin Summerfield, New York University*

In planning this new volume of the Series, the volume editors were motivated by the realization that, although the science of interior ballistics has advanced markedly in the past three decades and especially in the decade since 1970, there exists no systematic textbook or monograph today that covers the new and important developments. This volume, composed entirely of chapters written specially to fill this gap by authors invited for their particular expert knowledge, was therefore planned in part as a textbook, with systematic coverage of the field as seen by the editors.

Three new factors have entered ballistic theory during the past decade, each of which so happened from a stream of science not directly related to interior ballistics. First and foremost was the detailed treatment of the combustion phase of the ballistic cycle, including the details of localized ignition and flame spreading, a method of analysis drawn largely from rocket propulsion theory. The second was the formulation of the dynamical fluid-flow equations in two-phase flow form with appropriate relations for the interactions of the two phases. The third is what made it possible to incorporate the first two factors, namely, the use of advanced computers to solve the partial differential equations describing the nonsteady two-phase burning fluid-flow system.

The book is not restricted to theoretical developments alone. Attention is given to many of today's practical questions, particularly as those questions are illuminated by the newly developed theoretical methods. It will be seen in several of the articles that many pathologies of interior ballistics, hitherto called practical problems and relegated to empirical description and treatment, are yielding to theoretical analysis by means of the newer methods of interior ballistics. In this way, the book constitutes a combined treatment of theory and practice. It is the belief of the editors that applied scientists in many fields will find material of interest in this volume.

385 pp., 6 × 9, illus., \$25.00 Mem., \$40.00 List

TO ORDER WRITE: Publications Dept., AIAA, 1290 Avenue of the Americas, New York, N. Y. 10019